IFASD 2015
International Forum on Aeroelasticity and Structural Dynamics
June 28 — July 02, 2015 ▲ Saint Petersburg, Russia

AEROELASTIC MODELING AND SIMULATION OF FLEXIBLE JET TRANSPORT AIRCRAFT WITH HIGH-ASPECT-RATIO WINGS

Ryan C. Kitson[1] and Carlos E. S. Cesnik[2]

[1] Ph.D. Candidate, University of Michigan Aerospace Engineering Department
1320 Beal Ave, Ann Arbor, MI, 48104, USA
kitson@umich.edu

[2] Professor, University of Michigan Aerospace Engineering Department
1320 Beal Ave, 3024 FXB, Ann Arbor, MI, 48104, USA
cesnik@umich.edu

Keywords: nonlinear aeroelasticity, simulation, high-aspect-ratio wings.

Abstract: Future transportation aircraft requirements focused on energy efficiency and environmental impact are leading to design concepts with very high-aspect-ratio wings. These slender wings aim to maximize efficiency by reducing drag and lowering structural weight. The corresponding wing structures have larger structural deformations under aerodynamic loading and tighter coupling between the aeroelastic response and flight dynamics of the vehicle. Current engineering practice is to use linearized models for preliminary design of flight control and gust alleviation systems, but these models may not be able to capture nonlinearities in the vehicle response. The coupled aeroelastic and flight dynamic response of two aircraft designs were investigated to better understand the nonlinear aeroelastic implications of these future design trends. This paper reports the responses of two future configurations to control inputs and compares the results to linearized models. The linearized models are able to capture the structural and flight dynamic responses for moderate maneuvers and perturbations, but they show significant error for more aggressive maneuvers within the expected operating range.

NOMENCLATURE

C	Damping matrix
C^{GB}	Rotation matrix from the body frame to the global frame
f	Gust frequency
f_0	Lowest structural natural frequency
K	Stiffness matrix
K_λ	Constraint stiffness
M	Mass matrix
p_B	Global frame position of the body
q	Vehicle aeroelastic states (strain and body velocities)
Q_i	Coefficient matrices of the linearized system of equations ($i = 1, 2, 3$)
R	Residual force vector
R_λ	Constraint force residual
T	Gust period
t_0	Gust start time
t_f	Gust end time
u	Input perturbation vector
U_0	Gust downwash velocity amplitude

V_0 Cruise velocity
w Gust downwash velocity
x Linearized system perturbation state vector
y Linearized system dynamics vector
β Body frame velocities
δ Complex step size
λ Lagrange multiplier
δ_{surf} Control surface deflection (where *surf* can be aileron, elevator, rudder)
ε Beam strain
ζ Quaternions, global frame orientation of the body
Ω Quaternion coefficient matrix, which is a function of β
$\dot{(\cdot)}$ Time derivative
$\Delta()$ Perturbation about nonlinear equilibrium state

1 INTRODUCTION

Aviation technology must further develop to reduce the environmental impact of the growing air transportation industry. The FAA released industry forecasts that project significant growth in the number of revenue passenger miles (RPMs) for the fiscal years 2015-2035 [1]. Total mainline and regional RPMs are expected to increase by 1.7% on average domestically and 3.7% internationally with the highest growth expected in Latin America and Asia [1]. Local air quality, noise, and climate change are all negatively affected by the industry and those effects will intensify if there is not a significant change throughout the entire aviation system [2].

The FAA and NASA have developed technology programs, such as the Continuous Lower Energy, Emissions and Noise (CLEEN) program and the Subsonic Fixed Wing project, to promote technology development focused on energy efficiency and environmental impacts. At the system level, the NASA Subsonic Fixed Wing project focuses on energy efficiency in terms of vehicle aerodynamics, structures, and propulsion with specific technical challenges to reduce drag, structural weight, and fuel consumption [3]. These challenges have led to several lightweight and high-aspect-ratio wing designs aimed at increasing aerodynamic efficiency and structural weight simultaneously. However, these adjustments lead to flexible structures with large deformations and lower structural frequencies, which leads to interaction with the flight dynamics of the vehicle. Examples of this interaction have been shown for very flexible aircraft by Su and Cesnik for a flexible flying wing configuration in response to varying gust disturbances [4]. It is important to understand the coupling of the structural and flight dynamics of these high-aspect-ratio wing designs to maintain vehicle stability, safety, and maximize energy efficiency.

Flight control and gust alleviation systems are critical components to maintaining vehicle safety, but preliminary designs of these systems often depend on linearized models of the full vehicle that may not capture nonlinearities in a very flexible aircraft. In 2012, Dillsaver et al. [5] studied the linearized and nonlinear gust response of a flying wing configuration and showed that the linearized model may underestimate structural deformations and the flight dynamic response of the vehicle. Therefore, it is important to investigate the range of control inputs and gust intensities for future flexible designs to understand the applicable range of inputs for which the linearized model is an accurate and adequate representation of the full vehicle.

This paper addresses the nonlinear and linearized response of two vehicles representative of future aircraft design concepts that address energy efficiency to investigate the nonlinearities associated with these configurations and the ability of the linearized models to capture the nonlinear response. The configurations used in this study are shown in Figure 1 and based on the Common Research Model (CRM) and the Subsonic Ultra Green Aircraft Research (SUGAR) vehicle that were both developed by The Boeing Company. The CRM is a conventional tube and wing configuration with a flexible wing structure and the SUGAR model is a high-aspect-ratio wing design with truss bracing to support the wing structure. The numerical modeling and simulation of CRM and SUGAR were done within the University of Michigan Nonlinear Aeroelastic Simulation Toolbox (UM/NAST), which models the full vehicle in free flight. This toolbox allows us to capture nonlinear structural behavior due to large deformations and relative constraints critical to the chosen aircraft models. The full vehicle response is captured in UM/NAST by time-marching the coupled nonlinear aeroelastic and 6-DOF flight dynamics equations of motion. The CRM and SUGAR nonlinear and linearized models are simulated in response to control surface inputs and gust disturbances. These simulations highlight some of the nonlinear behavior and coupling between the aeroelastic and flight dynamic response. The nonlinear and linearized responses are compared for each case, emphasizing the accuracy of the linearized models in the expected range of surface deflections and gust disturbances.

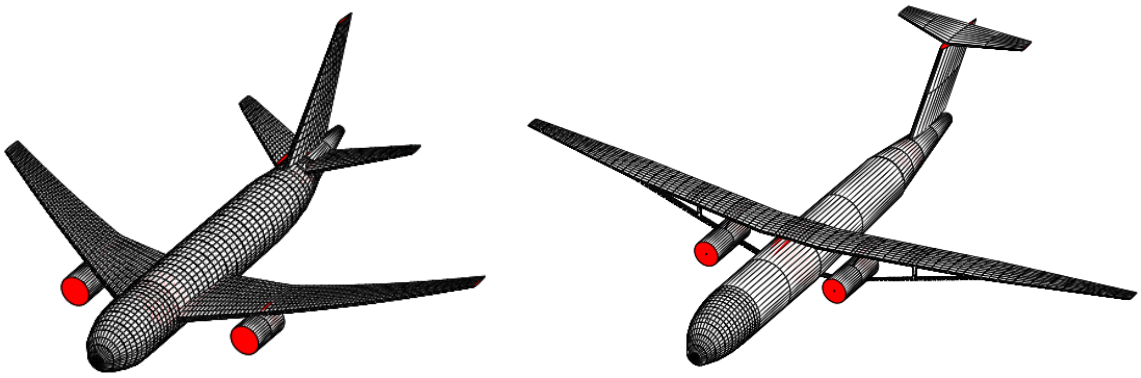

(a) CRM (b) SUGAR

Figure 1: UM/NAST Models of CRM and SUGAR concepts

2 METHODS

The primary tools used to analyze the CRM and SUGAR nonlinear and linearized model responses to control inputs and gust disturbances are described next. UM/NAST is the numerical framework used to model and analyze the aircraft in free flight using a coupled nonlinear set of equations for its aeroelastic and flight dynamics. The framework is based on a geometrically nonlinear beam finite element that can capture large deformations and joined-wing configurations. The method of segments [6] is a technique that is used to generate a reduced order aerodynamic model for flexible structures based on high-fidelity CFD data. This reduced order model (ROM) maintains accuracy for the given flight condition in a computationally efficient way. These ROMs were incorporated into the UM/NAST framework to provide the aerodynamic loads on the vehicle. The complex-step derivative [7]

is a numerical differentiation technique used to create the linearized models from the nonlinear set of equations. This method is an alternative to finite difference methods with improved accuracy and stability. Together, these methods led to the nonlinear and linearized results for the CRM and SUGAR vehicles studied here.

2.1 University of Michigan Nonlinear Aeroelastic Simulation Toolbox (UM/NAST)

UM/NAST is a computational framework that time marches the coupled aeroelastic system of equations for a vehicle in free flight using nonlinear beam finite elements to capture large deformations for very flexible structures [8]. This is accomplished by using a nonlinear strain-displacement relation and has been verified for static and dynamic structural loading by using NASTRAN as the reference solution [9]. A full aircraft is modeled in UM/NAST as a collection of the beam finite elements with structural and mass properties specified in the input file. Aerodynamic properties are defined by discretizing the lifting surfaces into span-wise sections and defining local aerodynamic properties for each section. This allows the user to define aerodynamic surrogates for each section as opposed to relying on a theoretical model. The nonlinear six degrees of freedom for the rigid body motion of the aircraft are coupled with the structural equations of motion and the coupled system is marched forward in time. For the cases studied here, the trapezoidal integration scheme was used. UM/NAST has previously been used to analyze various aircraft such as flying wing, blended-wing-body, and joined-wing configurations. Thus, UM/NAST is the proper tool to study the large deformations and relative constraints expected for CRM and SUGAR.

2.2 Method of Segments

The method of segments creates a surrogate aerodynamic model for the lifting surfaces of an aircraft based on high-fidelity CFD results that will approximate the loading on the elastically deformed vehicle. The method was introduced by Skujins and Cesnik [6] for reduced order aerodynamic modeling and has been added to the UM/NAST framework for this study. This method begins by running rigid CFD analysis on the aircraft wing at various flow conditions (Mach number and angle of attack). The wing is then divided into chord-wise segments and the pressure distribution for each segment is used to calculate the aerodynamic coefficients. Using this approach the deformed wing is viewed as a collection of rigid segments with unique local flow properties. This method is similar to a strip-theory approximation except that it includes the effects of flow in the span-wise direction.

Within UM/NAST the surrogate model generated by method of segments is represented by a Kriging surface for each wing segment. Kriging surfaces were chosen over other approximation techniques in anticipation of large structural deformations that might approach the boundaries of the set of CFD solutions. The inputs to the Kriging surface include the local angle of attack, Mach number and control surface deflection. The Kriging surface then outputs the approximate coefficients for lift, drag, and moment on the wing section. The result is a computationally efficient method of representing the CFD solution during the time marching analysis.

2.3 Complex-Step Differentiation

The complex-step derivative is an approximation that was used to generate the linearized system of equations for each aircraft configuration. The method, presented by Martins et al. [7], provides an accurate value for the derivative of a given function by avoiding cancellation error. Cancellation error is a well-known issue for numerical methods and commonly arises

for finite difference schemes as the step size is decreased. The complex-step derivative is given by:

$$\frac{\partial f}{\partial x} \approx \frac{\mathrm{Im}[f(x+ih)]}{h} \tag{1}$$

This provides an accurate approximation to the derivative of a function *f* by taking a finite forward difference in the complex plane. The basic form of the derivative was then applied to the nonlinear aeroelastic system of equations.

Using the complex-step derivative resulted in an accurate linearization for each aircraft model about the nonlinear equilibrium (trim) state of the vehicle for steady level flight. A trim state is the reference point commonly chosen for studying linear aircraft dynamics and developing control logic for the vehicle. The linearization process begins by calculating the nonlinear equilibrium state and arranging the vehicle states into a first order ordinary differential equation from the second order structural differential equation. Next, each state of the vehicle is perturbed with the complex step and the time derivative of the state vector is evaluated. The complex-step derivative represents the linearized contribution of each state to the time derivative of the state vector at equilibrium. Following this method one can obtain the linearized matrix equation by applying the same steps for the state vector, the first time derivative of the state vector, control inputs and gust disturbances. The assembled linearized system can then be integrated outside of UM/NAST using a time integration scheme such as Runge-Kutta. Two MATLAB routines were chosen for CRM and SUGAR to integrate the linearized equations of motion in response to the same inputs applied to the nonlinear system.

2.3.1 Problem Definition

The nonlinear problem is represented by the following second-order nonlinear aeroelastic system, one set of algebraic equations for the constraints, and two sets of first-order flight dynamics equations.

$$M\ddot{q} + C\dot{q} + Kq = R \tag{2}$$

$$K_\lambda \varepsilon = R_\lambda \tag{3}$$

$$\dot{\zeta} = -\frac{1}{2}\Omega\zeta \tag{4}$$

$$\dot{p}_B = C^{GB}\beta \tag{5}$$

$$q = \begin{Bmatrix} \varepsilon \\ \beta \end{Bmatrix}, \dot{q} = \begin{Bmatrix} \dot{\varepsilon} \\ \beta \end{Bmatrix}, \ddot{q} = \begin{Bmatrix} \ddot{\varepsilon} \\ \dot{\beta} \end{Bmatrix}$$

The result of the linearization is a first-order set of ordinary differential equations (ODE) with constant matrix coefficients representing the vehicle about a nonlinear equilibrium (trim) condition, that is:

$$Q_1\dot{x} = Q_2 x + Q_3 u \tag{6}$$

The state and input column vectors now contain perturbations of each state about the equilibrium point, and can be represented by:

$$x = \begin{Bmatrix} \Delta\varepsilon \\ \Delta\dot{\varepsilon} \\ \Delta\lambda \\ \Delta\beta \\ \Delta\zeta \\ \Delta p_B \end{Bmatrix}, \qquad u = \begin{Bmatrix} \Delta\delta_{aileron} \\ \Delta\delta_{elevator} \\ \Delta\delta_{rudder} \end{Bmatrix} \tag{7}$$

The matrices Q_1, Q_2, and Q_3 contain the constant linear coefficients of the governing ODE. To obtain Q_1 and Q_2, each state in x and $\dot{x}$ is perturbed in the complex plane according to the complex-step derivative. For each perturbation the following vector is calculated:

$$y = \begin{Bmatrix} \Delta\dot{\varepsilon} \\ \Delta\ddot{\varepsilon} \\ \Delta R_\lambda \\ \Delta\dot{\beta} \\ \Delta\dot{\zeta} \\ \Delta\dot{p}_B \end{Bmatrix} \tag{8}$$

The beam strain rate perturbation $\Delta\dot{\varepsilon}$ is taken directly from the input vector x. The beam strain acceleration perturbation $\Delta\ddot{\varepsilon}$ and body frame acceleration perturbation $\Delta\dot{\beta}$ come from solving the equations of motion in Eq. (2). The perturbation of the Lagrange constraint residual R_λ is obtained by Eq. (3). The orientation and position of the vehicle in the global frame is represented by the quaternion states ζ and position vector p_B. The perturbations of the global frame orientation and position rates are obtained from Eqs. (4) and (5).

The column of Q_1 and Q_2 associated with the perturbed state is calculated by the complex-step derivative shown in Eq. (1), that is:

$$Q_j = \frac{\mathrm{Im}(y)}{\delta} \tag{9}$$

The vector y is equal to $\dot{x}$ except ΔR_λ replaces $\Delta\dot{\lambda}$, which is a non-physical quantity. Each column of Q_3 is obtained by perturbing the corresponding input about the equilibrium value.

2.3.2 Pseudo Code

The linearization process has been implemented as a loop over all of the vehicle states and state rates. During each iteration one degree of freedom is perturbed by a very small amount in the complex direction. The vehicle state is updated and the vehicle loads are calculated based on the new state. The equations of motion can then be solved to obtain the quantities listed in vector y. Calculating the derivative using the vector y yields the column of Q_j associated with the perturbed state degree of freedom, that is:

```
for j = 1:(num of states)*2
    xx = [x; xdot]
    xx(j) = xx(j) + √-1 *DEL
    Update the vehicle state (UM/NAST)
    Update the vehicle loads (UM/NAST)
    Solve for y (UM/NAST)
```

```
    Q(:,j) = Im(y)/DEL
end
Q2 = Q(:,1:n)
Q1 = Q(:,n+1:end)

for j = 1:(num of inputs)
      uu(j) = uu(j) + sqrt(-1) *DEL
      Update vehicle loads (UM/NAST)
      Solve for y (UM/NAST)
      Q3(:,j) = Im(y)/DEL
end
```

2.3.3 Integration

The result of this linearization process is an equation in the form of Eq. 6 that is integrated outside of UM/NAST using MATLAB integration functions. For CRM, `ode15s` was chosen because of its robustness and capability of handling a mass matrix, which is represented in this problem by Q_1. The MATLAB function `ode15i` is used for the SUGAR model, which solves the implicit equation $0 = f(x,\dot{x},u)$ and integrates the state vector over time. This function was chosen specifically to handle the differential algebraic equation as opposed to the function used for CRM. The system of equations for the linearized model, Eq. (6), can be rearranged into the implicit form as:

$$0 = Q_1\dot{x} - Q_2 x - Q_3 u \tag{10}$$

3 NUMERICAL MODELING

Detailed structural and aerodynamic models of the CRM and SUGAR have been documented by Vassberg et al. [10] and Bradley et al. [11, 12], respectively. The available information for each model was adapted for the UM/NAST beam finite element framework. The structural and aerodynamic properties for the wing structure were used to model the flexible sections of the vehicle. The fuselage and empennage were modeled as a rigid structure with one rigid-body mass to represent the total weight and inertia. The engine was modeled as a rigid structure with a point mass attached to the wing, but was modeled without any aerodynamic properties. These approximations were based on simplifying the analysis and to focus only on the wing structure, which was expected to be the most critical component to any nonlinear behavior. The structural and aerodynamic data compose the numerical model used in UM/NAST for all of the nonlinear simulations and used to define the nonlinear equilibrium point to create the linearized models.

3.1 Properties of the Common Research Model

The numerical model of the CRM is based on the vehicle developed in [10][1]. CRM was designed to be representative of contemporary commercial transport aircraft and used as a common test case for CFD and experimental studies. It was chosen for this study as a representative geometry of current cantilevered wing designs and for the opportunity to compare results to future aeroelastic studies.

[1] It is publicly available at http://commonresearchmodel.larc.nasa.gov/

The geometry of the UM/NAST CRM model shown in Figure 2 uses the CRM wing structure in conjunction with a fuselage and empennage loosely based on a B777 class aircraft. The wings are the only flexible members of the model and the structural and mass properties are defined in Figure 3 as well as the free vibration results in Table 1. The flexible elements along the wing contribute the elastic degrees of freedom contained in the state vector. Table 2 lists the finite element breakdown of the state vector used for the linearized model. The aileron is modeled as the last 25% span and 25% chord of the wing. The elevator and rudder span 100% of the horizontal and vertical stabilizers and are both 25% chord.

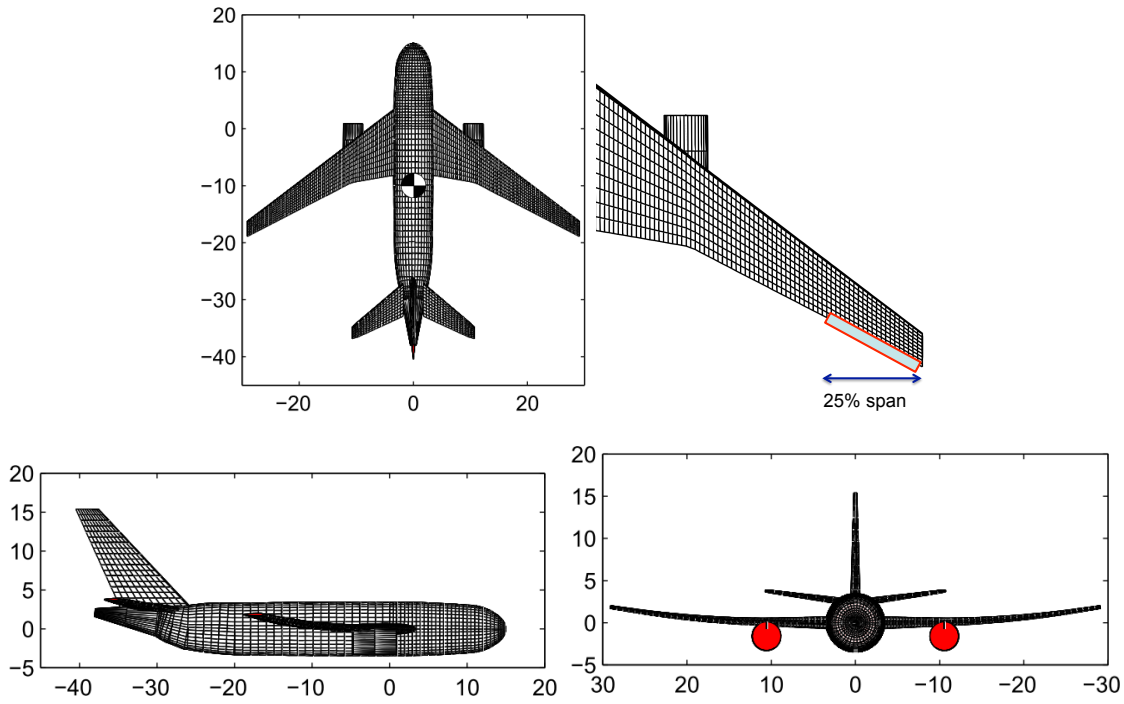

Figure 2: Geometric definition of the CRM model in UM/NAST (units: meters)

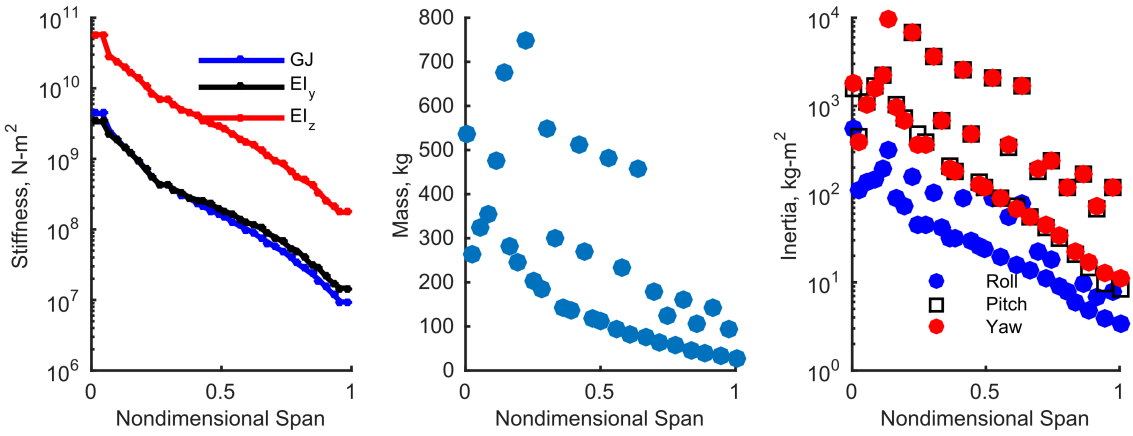

Figure 3: Structural property distribution for the CRM wing

The University of Michigan Multidisciplinary Design Optimization (MDO) Laboratory used the geometry of the CRM wing to obtain surface pressures from CFD solutions of the Navier-Stokes equations. The CFD solutions at various Mach numbers and angles of attack of the rigid 1*g* wing shape were used to create the surrogate models using the method of segments

and Kriging surface approximation. The accuracy of the Kriging surfaces is exemplified in Figure 4 for various angles of attack at the design cruise Mach number. To test the method of segments, the aerodynamic surrogate model was used to compare the loading on a deformed wing shape. This measures how well the method of segments approximates the aerodynamic loads for a shape away from the shape used to generate the surrogate model. A comparison of the surrogate model and a CFD solution of the deformed shape is shown in Figure 5. The overall correlation for this deformed wing indicates the appropriateness of the model to predict the loads during the time simulation for moderate deformations.

Table 1: Vibration frequencies of the CRM and SUGAR unloaded wing structures

	CRM Frequency, Hz (UM/NAST)	SUGAR Frequency, Hz (UM/NAST)	SUGAR Frequency, Hz (Ref [15])
1st Out of Plane Bending	1.23	2.24	5.04
2nd Out of Plane Bending	4.00	5.14	8.44
1st In Plane Bending	4.93	2.82	5.70
1st Torsion	9.33	7.95	11.3

Table 2: Finite element details of the CRM and SUGAR models

	CRM	SUGAR
Total number of elements	143 (72 flexible)	150 (126 flexible)
Total number of elastic states, ε (4 per flexible element)	288	504
Body frame velocity states, β	6	6
Global frame position states, ζ and p_B	13	13
Relative constraint states, λ	0	18
Total number of vehicle states	589	1045

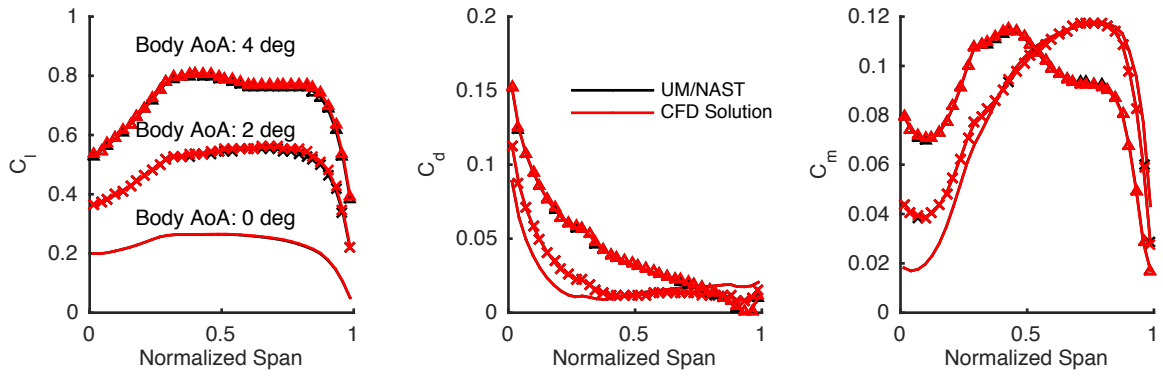

Figure 4: CRM aerodynamic surrogate model comparison to CFD data for the 1g wing shape

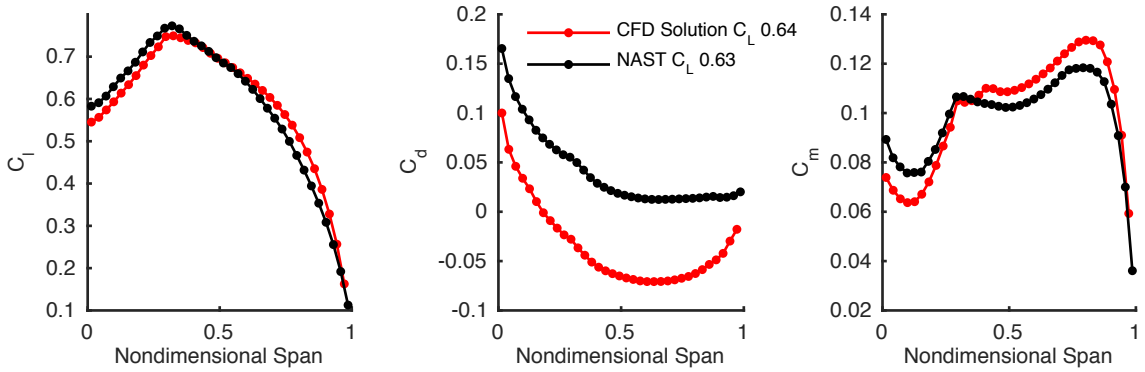

Figure 5: CRM aerodynamic surrogate model comparison to CFD data for the 2.5g deformed shape

All other properties of the vehicle regarding the fuselage, engines, and empennage were based on a B777-200ER aircraft, which is similar in size to the CRM. The flight conditions used for the CRM simulations are given in Table 3. The cruise altitude and velocities were based on the design conditions presented in [10]. The vehicle weight was based on aircraft design estimate methods for this class of aircraft [11]. These quantities were used within UM/NAST to calculate the angle of attack, thrust, and elevator deflection for trimmed level flight.

Table 3: CRM and SUGAR flight conditions

	CRM	SUGAR
Altitude, km	10.9	13.8
Velocity, m/s	254	216
Mach	0.85	0.73
Cruise angle of attack, deg	3.24	3.57

3.2 Properties of the SUGAR model

The numerical model of SUGAR is based on the vehicle developed by The Boeing Company as part of the NASA Subsonic Fixed Wing project [11, 12]. The vehicle features a very high-aspect-ratio wing (aspect ratio 19.55) and truss-braced design. This design is driven by maximizing aerodynamic efficiency of the wing to improve overall energy efficiency of the vehicle.

The geometry of the UM/NAST SUGAR model is shown in Figure 6 following the information contained in [11, 12]. The structural properties of the wing, strut, and jury shown in Figure 7 were provided in terms of beam properties that are used directly in the UM/NAST finite element framework. The free vibration results of the wing structure are listed in Table 1. The elevator and rudder control surfaces are modeled as 100% span and 25% chord of the horizontal and vertical stabilizers, respectively. The aileron and inboard trailing edge surfaces are specified in Figure 6.

Table 4: Mass and inertia properties of the CRM and SUGAR models

	CRM	SUGAR
Vehicle Mass, kg	$2.009\ 10^5$	$5.773\ 10^4$

Vehicle Inertia, kg-m^2		
Pitch	4.306 10^6	2.241 10^6
Pitch-Roll	-0.5031	1.490 10^{-11}
Pitch-Yaw	8.519 10^{-3}	2.130 10^{-9}
Roll	5.004 10^6	2.645 10^6
Roll-Yaw	-6.458 10^4	5.596 10^4
Yaw	9.228 10^6	2.865 10^6
Engine Mass, kg	7559	3559
Engine Inertia, kg-m^2	N/A	
Pitch		3669.7
Roll		1672.1
Yaw		3262.9

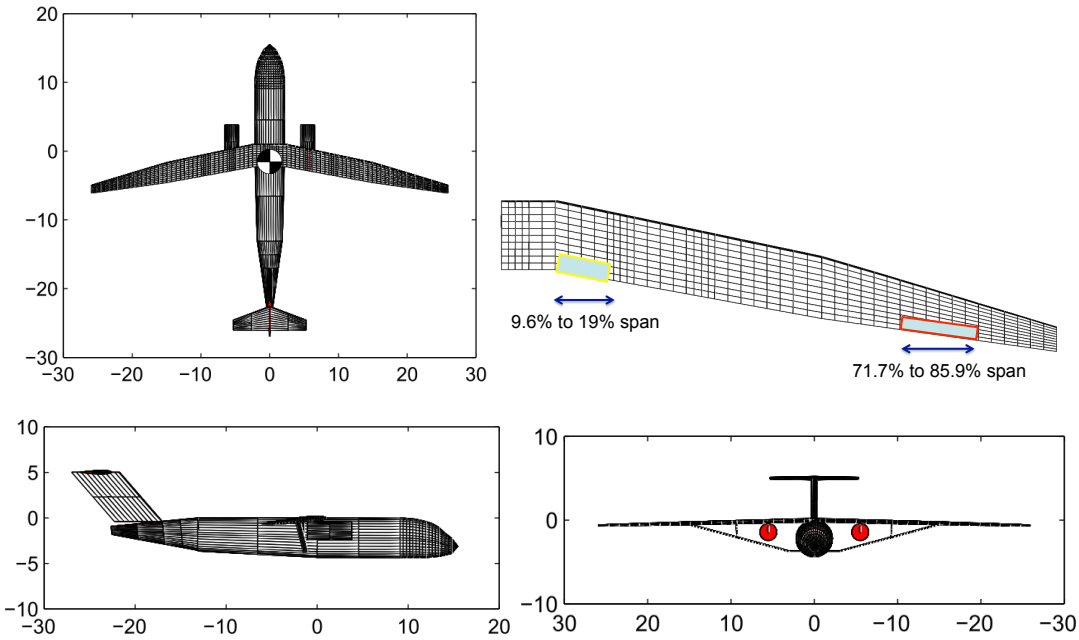

Figure 6: Geometry definition of the SUGAR model (units: meters)

The aerodynamic properties for the wing were provided as sectional aerodynamic coefficients from CFD solutions that could be used as the input for the method of segments to create the aerodynamic surrogate model. The aerodynamic loading on the wing is shown in Figure 8 at two design points.

The flight conditions used for the simulations are listed in Table 3. The cruise altitude, velocities, and total weight were based on the design conditions presented in [12]. These quantities were used within UM/NAST to define the SUGAR flight conditions and calculate the trim state. The mass and inertia properties of the rigid fuselage and engine components are in Table 4.

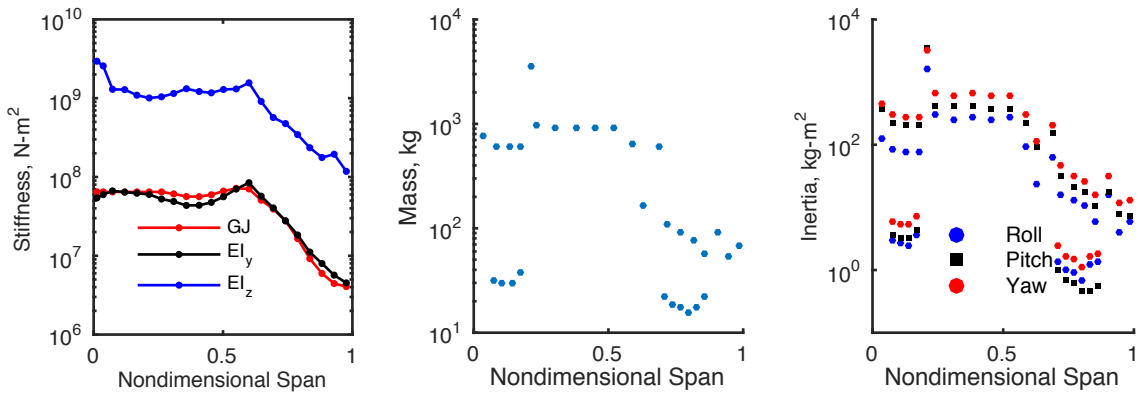

(a) Wing Properties

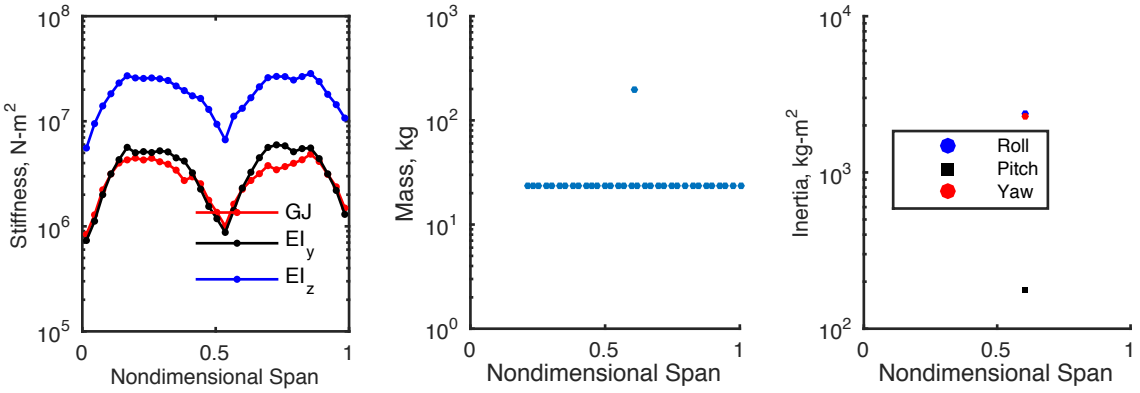

(b) Strut Properties

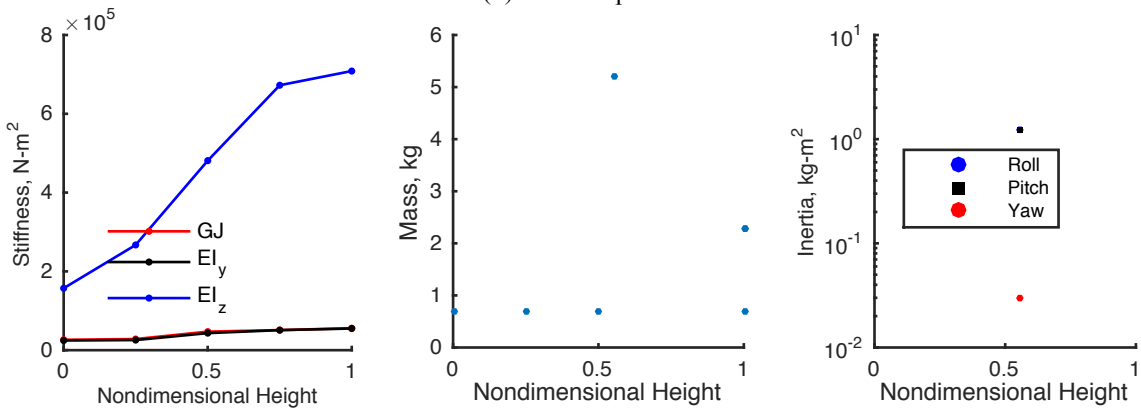

(c) Jury Properties

Figure 7: Structural property distribution of the SUGAR wing structure

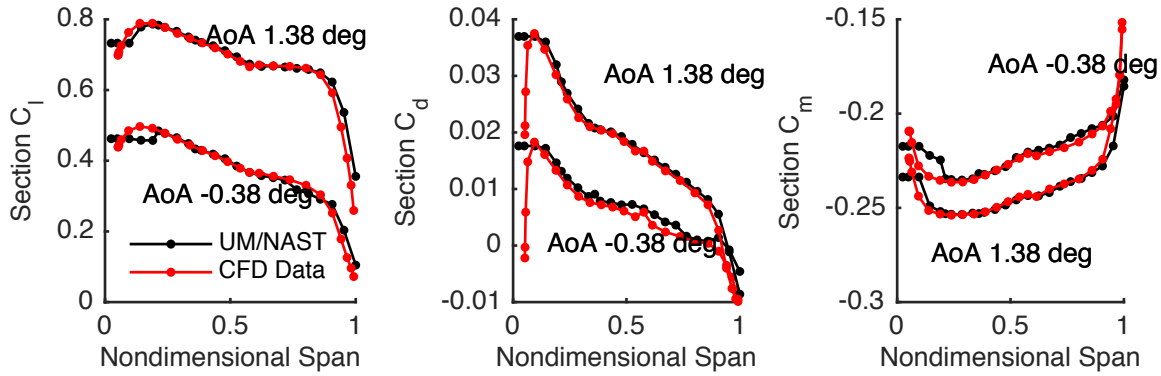

Figure 8: Aerodynamic load distribution of the SUGAR wing

4 RESULTS

The structural and aerodynamic properties used to create the low-order UM/NAST models matches the high-fidelity solutions in general for CRM and SUGAR. There is a significant difference between the UM/NAST calculated free vibration results for SUGAR compared to the results in [15]. The UM/NAST vibration frequencies are significantly lower than the reference values for the lowest bending and torsion modes of the wing structure. This is attributed to changes in the finite element model stiffness and/or mass properties as the SUGAR study progressed at NASA/Boeing. The data used here is from an original model from that study. This difference, however, does not impact the studies conducted here on the effects of the linearization of the coupled nonlinear aeroelastic/flight dynamics representation of the flexible aircraft.

The SUGAR and CRM responses to a gust disturbance and aileron control inputs were investigated, respectively, for the nonlinear and linearized models. The control surface input time history was chosen to be representative of an actual pilot command as opposed to a step function. Similarly, the gust characteristics were chosen to be as simple as possible to minimize the complexity of the response. The structural response for each simulation is represented by the wing tip deflection and the out-of-plane bending strain at the wing root. These parameters illustrate the loading and deformation on the vehicle during the simulation. The vehicle linear and rotational velocities in the body frame are presented along with the vehicle inertial frame position and orientation to compare the rigid-body degrees of freedom and flight dynamics of the vehicle. These parameters represent the observable vehicle states available for a control system. For each disturbance and input case, the same time history profile was varied in magnitude to get an error profile for the linearized model. These plots provide information regarding the range of disturbances and inputs for which the linearized model is applicable.

4.1 SUGAR Gust Response

The gust model used in this study is the uniform “1-cos” model. The gust intensity was chosen to be a specific fraction of the vehicle forward velocity and the gust frequency was chosen based on the lowest structural natural frequency. Table 5 shows the chosen gust parameters used during the simulation.

Table 5: Simulated gust parameters

Downwash	$w(t) = U_0 / 2(1 - \cos(2\pi(t - t_o)/T))$
U_0	$V_0 / 10 = 216/10 = 21.6$ m/s
f	$f_0 / 2 = 2.24/2 = 1.12$ Hz
T	$1/f$
t_0	0.5 s
t_f	$t_0 + T$

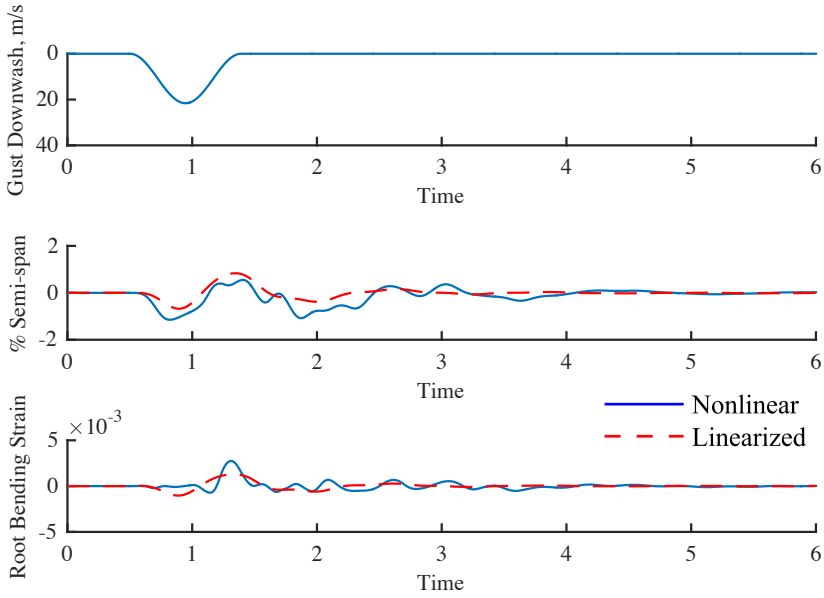

Figure 9: Structural response of the SUGAR models to a gust disturbance

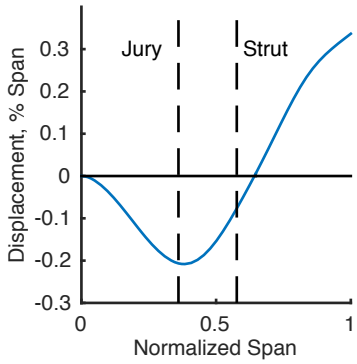

Figure 10: Vertical wing displacement of the nonlinear model during peak root bending strain

The structural response of the SUGAR model to the gust disturbance is shown in Figure 9 and reveals some significant differences between the linearized and nonlinear models. The nonlinear model shows a very high frequency response with larger amplitudes compared to the linearized model. The larger root bending strain is due to the loss of stiffness of the inner wing between the fuselage and jury connection from the compressive loads. The bending strain peak near 1.25 seconds into the simulation corresponds to a concave-up shape for the

inner wing and a positive tip deflection shown in Figure 10. The nonlinear strain response shows that the inner wing does not deform much during negative tip deflections. These phenomenon suggest that the strut and jury supports have a significant effect on the response that is not being represented by the linearized model.

The flight dynamic response to the gust disturbance, in Figure 11 and Figure 12, shows very good correlation between the two models in the body frame and the pitch angle in the inertial frame. Therefore despite the differences in structural response, the linearized model is capturing the flight dynamics of the vehicle reference system well. The nonlinear model inertial frame velocity in Figure 12 is significantly different than the linearized model and can be understood by looking at the lift-to-weight ratio of the vehicle about the nonlinear equilibrium point shown in Figure 13. These results show that the linearized model is actually overestimating the lift-to-weight ratio since it is not considering the further inboard rotation of the aerodynamic force that reduces the effective lift. This explains why the linearized model is not losing altitude relative to the nonlinear model.

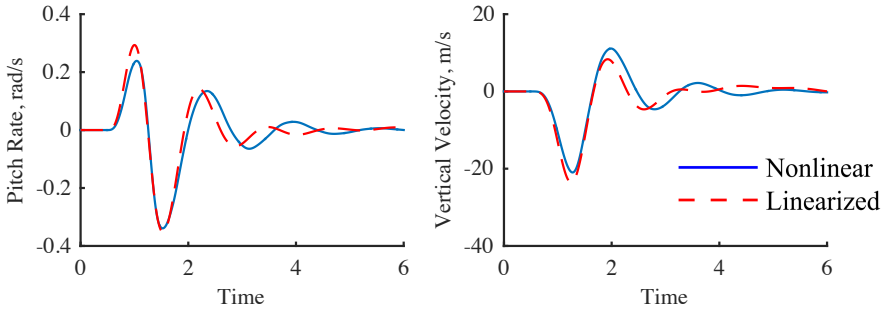

Figure 11: Body frame flight dynamics response of the SUGAR models to a gust disturbance

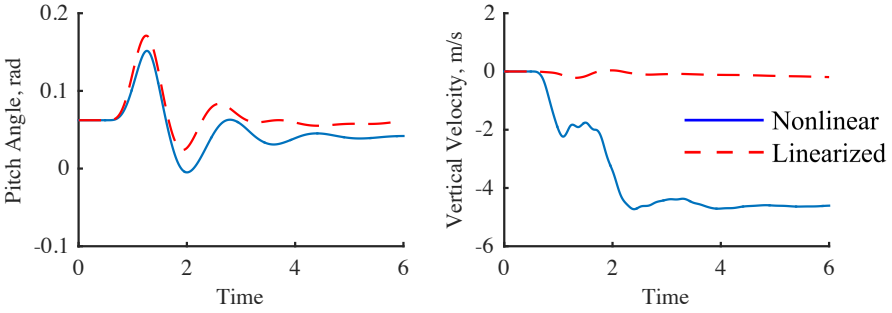

Figure 12: Global frame flight dynamics response of the SUGAR models to a gust disturbance

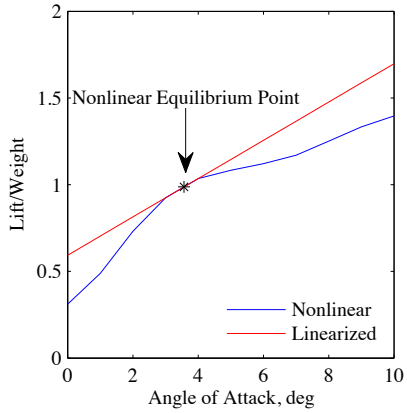

Figure 13: Lift-to-weight ratio of the SUGAR linearized and nonlinear models at the cruise velocity and altitude

4.2 CRM Aileron Command

Consider the structural response of the CRM aircraft due to an aileron command. The strain state and tip deflection of the right wing for the linearized and nonlinear models are shown in Figure 14. The nonlinear model shows some higher frequency response, but the overall amplitude and response of the linearized model closely matches the nonlinear response. The amplitude of the fluctuations are relatively small and do not affect the overall behavior of the vehicle.

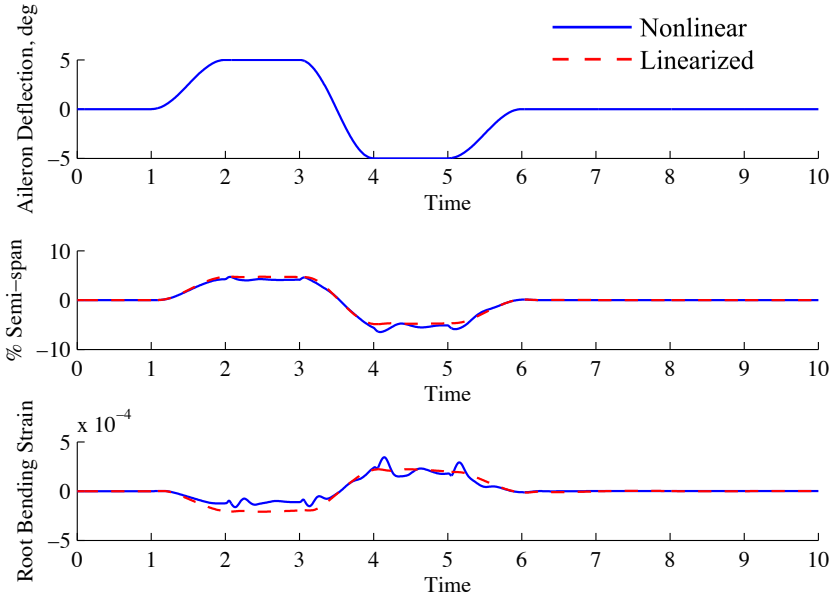

Figure 14: Structural response of the CRM models to an aileron input

The flight dynamic rotational and translational velocities are shown in Figure 15 and 16 for both models in the body and global frames, respectively. The correlation between the linearized and nonlinear model is not as strong as the elastic degrees of freedom, but the overall behavior is similar. This is an example of the linearized model providing qualitative information that is useful to understanding the basic response of the vehicle. The global frame lateral velocity of the linearized model shows an initial trend in the opposite direction and then reverses. Figure 17 highlights the first two seconds of the response and it shows this behavior is an amplification of the trend showed in the nonlinear model for very small aileron deflections. This causes a significant time delay on the lateral velocity response to aileron command that can be an issue in control stability. This time delay is due to the inboard transfer of aerodynamic loads due to wing deformation leading to a loss in controllability.

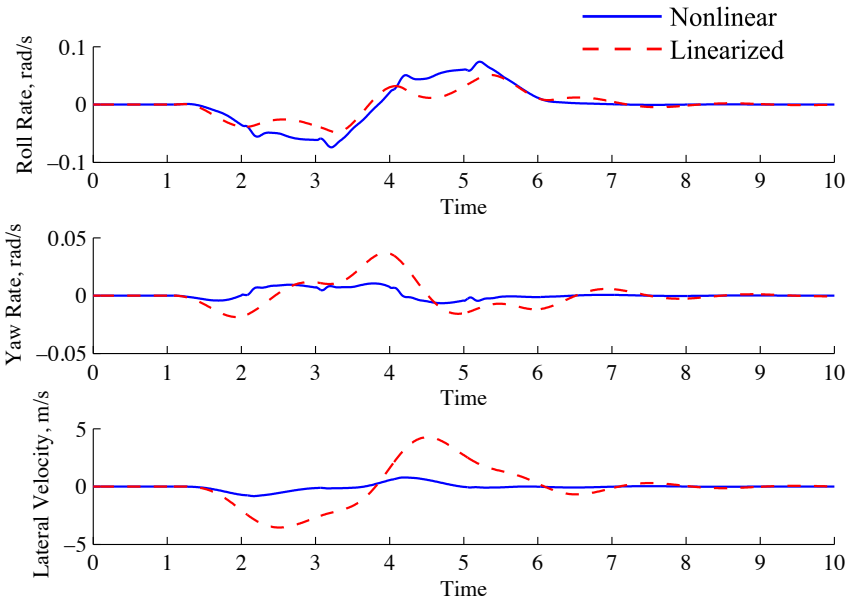

Figure 15: Flight dynamics response (body frame) of the CRM models to an aileron input

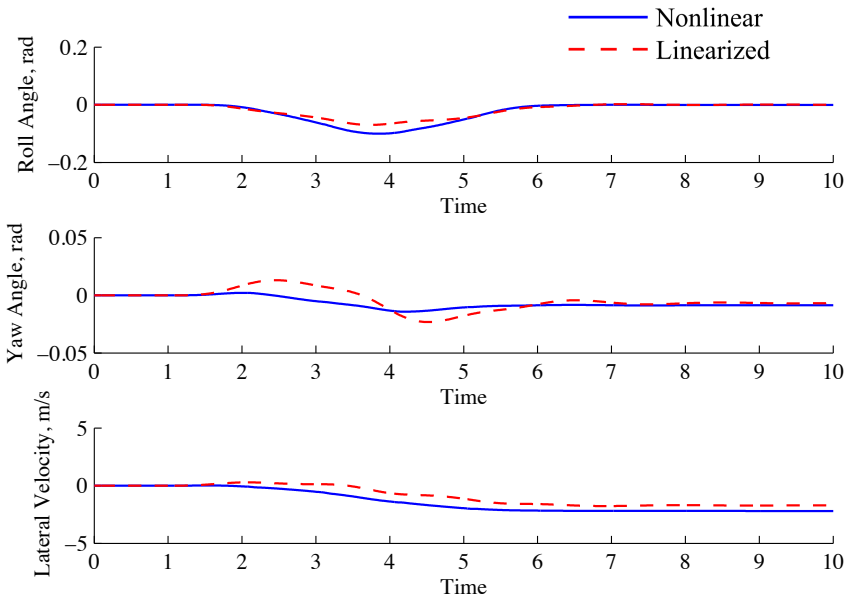

Figure 16: Flight dynamics response (global frame) of the CRM models to an aileron input

Linearized models offer some significant advantages such as computational time and complexity. However, it is important to understand the bounds for which the linearized model is accurately representing the overall behavior of the vehicle. Beyond these bounds, the nonlinear model should be used to qualitatively study the vehicle response. The evolution of this error is shown in Figure 18. For roll maneuvers with maximum roll rates beyond 10 deg/s the absolute tip deflection error is greater than 1% semi-span and the maximum error in roll rate is greater than 0.1 rad/s (≈ 5.7 deg/s). Around 14 deg/s of maximum roll rate, the two error metrics grow significantly, reaching 10% semi-span and 0.4 rad/s (≈ 23 deg/s), respectively.

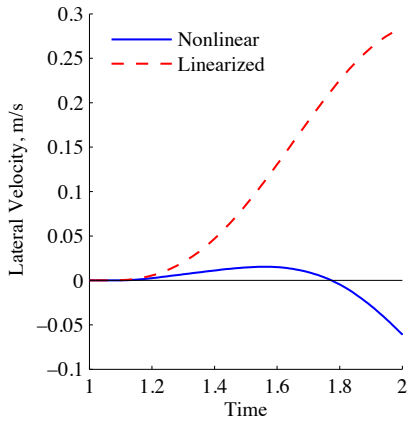

Figure 17: The global frame dynamics of the CRM models at the beginning of an aileron input

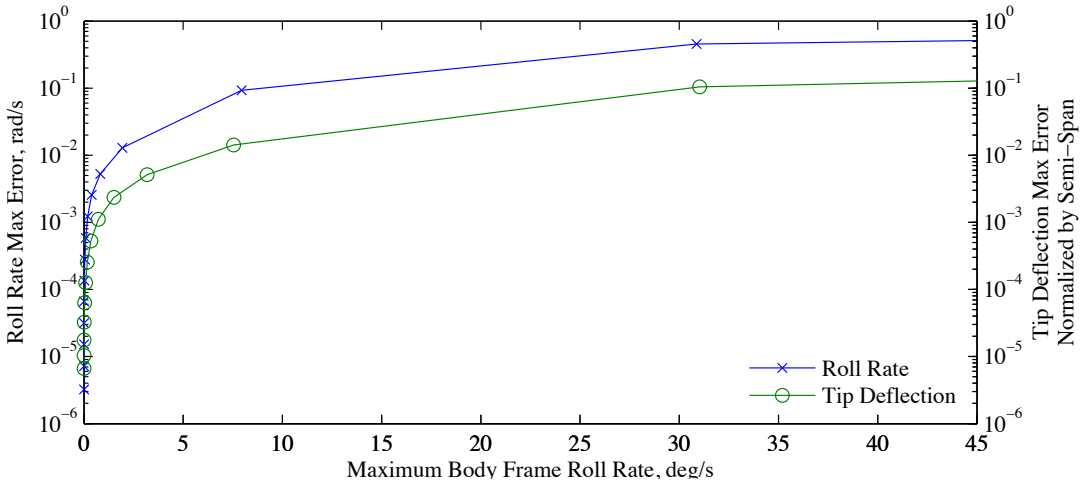

Figure 18: Error due to linearization over the expected range of aileron inputs

5 CONCLUDING REMARKS

This paper has focused on the open-loop response of a nonlinear and linearized set of models for two aircraft configurations representative of future energy efficient designs. The nonlinear model couples the aeroelastic equations with the rigid body equations in the time domain. The linearized model is calculated about the trim state of the nonlinear model. Examples were presented for a gust disturbance and aileron command. Based on these simulations nonlinear aeroelastic behavior was observed for each model within the operational range of inputs to the system. The SUGAR inner wing structure showed nonlinear behavior due to the stiffness of the strut and jury support causing a loss of stiffness along the inner wing. The CRM model showed nonlinear aeroelastic behavior as a reduction in roll control authority due to the wing bending deformation (about 5% semi-span) and inboard transfer of loads induced by the aileron deflection.

The nonlinear and linearized solutions provide evidence to the fact that high-aspect-ratio-wing transport aircraft contain nonlinearities in the system and a linearized model may be unable to capture these effects. Both CRM and SUGAR nonlinear models show higher frequency structural response that was not reflected in the linearized models. Therefore more complex or aggressive maneuvers can excite additional nonlinear structural responses that will not be captured accurately by the linearized models. The linearized models show significant error for the structural and flight dynamics degrees of freedom beyond a certain

level of disturbance or input. For both configurations, this threshold appears within the expected operational range of the vehicle, which suggests that the linearized model should not be used for the entire range. Instead, the linearized models could be used to investigate the fundamental behavior of each configuration to design the logic behind a control system and refine any control parameters or gains with the nonlinear model. Beyond the preliminary design phase the fully nonlinear model should be used to refine the control system parameters throughout the operational range of inputs and gust disturbances.

The nonlinear solutions for CRM show that the aeroelastic and flight dynamic response is generally well captured by the linearized model. However, there exists nonlinearity in the aileron input case. The linearized model shows significant differences due to the wing flexibility leading to a nonlinear flight dynamics response. The wing flexibility leads to an adverse yaw effect that is exaggerated in the linearized model, but is less pronounced in the nonlinear model. This leads to a reduction in control authority for aileron deflections within the expected range of operation. The aeroelastic and flight dynamics error in the linearized model becomes significant when the body frame roll rate for maneuvers is greater than 2 deg/s, a very small rate. This is reflected as a large phase delay in the lateral velocity response to the aileron input.

The SUGAR results show that the linearized model does not accurately represent the structural response to a gust disturbance. This is due to the nonlinear interaction between the strut and jury bracing and the inner wing. The strut and jury cause the inner wing to lose bending stiffness during positive tip deflections and limit any inner wing deformation during negative tip deflections. This results in the linearized model underestimating peak loads at the wing root.

The results obtained for the CRM and SUGAR models emphasize the fact that one should expect nonlinearities in the coupled aeroelastic and flight dynamics response of very flexible transport aircraft, including truss-braced wings. This suggests that nonlinear modeling capability is critical in developing a thorough understanding of the aeroelastic behavior for flexible and efficient aircraft configurations.

6 AKNOWLEDGMENTS

The authors would like to thank the Multidisciplinary Design Optimization Laboratory at the University of Michigan for the CFD contributions to this work. This work was supported by the Subsonic Fixed Wing Program with Dr. Irene Gregory as the technical monitor. Opinions, interpretations, conclusions, and recommendations are those of the authors and are not necessarily endorsed by the United States Government.

7 REFERENCES

[1] Anon., "FAA Aerospace Forecast Fiscal Years 2015-2035," Federal Aviation Administration, 2015.

[2] I. Waitz, J. Townsend, J. Cutcher-Gershenfeld, E. Greitzer and J. Kerrebrock, "Report to the United States Congress: Aviation and the Environment," Partnership for Air Transportation Noise and Emissions Reduction (PARTNER), 2004.

[3] D. M. Acosta, M. D. Guynn, R. A. Wahls and R. D. Rosario, "Next Generation Civil Transport Aircraft Design Considerations for Improving Vehicle and System-Level Efficiency," in *2013 Aviation Technology, Integration, and Operations Conference*, 2013.

[4] W. Su and C. E. S. Cesnik, "Dynamic Response of Highly Flexible Flying Wings," *AIAA Journal,* vol. 49, no. 2, pp. 324-339, 2011.

[5] M. J. Dillsaver, C. E. S. Cesnik and I. V. Kolmanovsky, "Trajectory Control of Very Flexible Aircraft with Gust Disturbance," in *AIAA Atmospheric Flight Mechanics Conference*, AIAA 2013-4745, 2013.

[6] T. Skujins and C. E. S. Cesnik, "Reduced-Order Modeling of Unsteady Aerodynamics Across Multiple Mach Regimes," *AIAA Journal of Aircraft,* vol. 51, no. 6, pp. 1681-1704, 2014.

[7] J. R. R. A. Martins, P. Sturdza and J. J. Alonso, "The Complex-Step Derivative Approximation," *ACM Transactions on Mathematical Software,* vol. 51, pp. 245-262, 2003.

[8] C. E. S. Cesnik and W. Su, "Nonlinear Aeroelastic Modeling and Analysis of Fully Flexible Aircraft," in *46th AIAA/ASME/ASCE/AHS/ASC Structures, Structural Dynamics and Materials Conference*, AIAA 2005-2169, 2005.

[9] W. Su, "Coupled Nonlinear Aeroelasticity and Flight Dynamics of Fully Flexible Aircraft," Ph.D. Dissertation, University of Michigan, Ann Arbor, 2008.

[10] J. C. Vassberg, M. A. DeHaan, S. M. Rivers and R. A. Wahls, "Development of a Common Research Model for Applied CFD Validation Studies," in *26th AIAA Applied Aerodynamics Conference*, AIAA 2008-6919, 2008.

[11] J. Roskam, Airplane Design Part V: Component Weigth Estimation, Design, Analysis and Research Corporation, Lawrence, Kansas, 2003.

[12] M. K. Bradley and C. K. Droney, "Subsonic Ultra Green Aircraft Research: Phase I Final Report," NASA Langley Research Center, Hampton, NASA/CR-2011-216847, 2011.

[13] W. Su and C. E. S. Cesnik, "Nonlinear Aeroelasticity of a Very Flexible Blended-Wing-Body Aircraft," *AIAA Journal,* vol. 47, no. 5, pp. 1539-1553, 2010.

[14] R. E. Bartels, R. Scott, T. J. Allen and B. W. Sexton, "Aeroelastic Analysis of SUGAR Truss-Braced Wing Wind-Tunnel Model Using FUN3D and a Nonlinear Structural Model," in *56th AIAA/ASCE/AHS/ASC Structures, Structural Dynamics and Materials Conference*, AIAA 2015-1174, 2015.

[15] C. V. Jutte, B. K. Stanford, C. D. Wieseman and J. B. Moore, "Aeroelastic Tailoring of the NASA Common Research Model via Novel Material and Structural Configurations," in *52nd Aerospace Sciences Meeting*, AIAA 2014-0598, 2014.

[16] M. K. Bradley and C. K. Droney, "Subsonic Ultra Green Aircraft Research: PhaseII: N+4 Advanced Concept Development," NASA Langley Reserach Center, Hampton, NASA/CR-2012-217556, 2012.

8 COPYRIGHT STATEMENT